IEEE Access
Multidisciplinary | Rapid Review | Open Access Journal

Received March 14, 2021, accepted March 26, 2021, date of publication March 30, 2021, date of current version April 6, 2021.

Digital Object Identifier 10.1109/ACCESS.2021.3069821

Practical Aspects of the Skin Effect in Low Frequencies in Rectangular Conductors

SÉRGIO H. L. CABRAL[1], SÁVIO L. BERTOLI[2], ALESSANDRO MEDEIROS[1], CRISLEINE REGINA HILLESHEIM[2], CAROLINA K. DE SOUZA[2], STÉFANO FRIZZO STEFENON[3], (Graduate Student Member, IEEE), ADEMIR NIED[3], (Member, IEEE), VALDERI REIS QUIETINHO LEITHARDT[4,5], (Member, IEEE), AND GABRIEL VILLARRUBIA GONZÁLEZ[6]

[1]Electrical Engineering Graduate Program (PPGEE), Electrical Engineering Department, Regional University of Blumenau (FURB), Blumenau 89030-000, Brazil
[2]Chemical Engineering Graduate Program (PPGEQ), Chemical Engineering Department, Regional University of Blumenau (FURB), Blumenau 89030-000, Brazil
[3]Electrical Engineering Graduate Program, Electrical Engineering Department, Santa Catarina State University (UDESC), Joinville 89219-710, Brazil
[4]VALORIZA-Research Centre for Endogenous Resource Valorization, Polytechnic Institute of Portalegre (IPP), 7300 Portalegre, Portugal
[5]COPELABS, Universidade Lusófona de Humanidades e Tecnologias, 1749-024 Lisboa, Portugal
[6]Expert Systems and Applications Laboratory, Faculty of Science, University of Salamanca, 37008 Salamanca, Spain

Corresponding author: Stéfano Frizzo Stefenon (stefano.stefenon@udesc.br)

This work was supported by Junta De Castilla y León—Consejería De Economía Y Empleo: System for simulation and training in advanced techniques for the occupational risk prevention through the design of hybrid-reality environments under Grant J118.

ABSTRACT Although the skin effect has been widely studied over the years, many of its topics remain unclear for most electrical engineers, including undergraduate students and fresh graduates. Yet, in the cases of application of power frequency current, the knowledge gap to be bridged is more significant. Thus, for contributing to the widening in the knowledge of this effect, this work presents an analysis of the behavior of the current density distribution over the cross-section of differently combined rectangular conductors subject to power frequency current. In this case, since an analytical approach is not feasible, the numerical method of matrix solution of integral equations was adopted due to its simplicity, fast convergence, and its application is presented through some providentially chosen theoretical examples before a practical case may be analyzed. As the main results, the influence of a correlated effect that is the proximity effect shows itself as being predominant and the method presents itself as being very convenient for studying the current density distribution in conductors with a cross-section other than the circular, which allow bridging the knowledge gap in this theme. Moreover, the comparison of theoretical cases quite significant. Moreover, the method is adequate to planar configurations, by typical configurations, as in the case of bus bars of electrical panels.

INDEX TERMS Numerical modeling, power frequency, proximity effect, rectangular conductor, skin effect.

I. INTRODUCTION

As already properly pointed out in [1], the importance and the complexity of the skin effect justify this as being that kind of theme to be regularly revisited, which explains why it has been under investigation for more than a century [2]. Specifically, regarding this effect under power frequency, its ever-growing importance is represented by many published works that show the key role played by this effect in designing some vital high-current equipment of power systems as power substation bus bars [3], induction motor rotor bars [4] and medium voltage panel bus bars [5], [6].

Moreover, this effect is a very important concern in designing low power and electronic equipment as shown in [7] and [8], [9], for example. Regarding high-current equipment, for most of them, the geometry of the adopted conductors is rarely circular [10], [11]. Thus, although it is only for the circular conductor that a relatively well-known and diffused classical analytical approach for the skin effect exists, practical and other reasons make this geometry not prevailing as adopted but mostly the rectangular besides other non-regular geometries [12].

Moreover, the classical analysis for the circular conductor is valid only for the case of an isolated conductor, which is also rarely found in practical applications. Indeed, because of the mutual influences of inherently close conductors in practical arrangements, another effect assumes the

The associate editor coordinating the review of this manuscript and approving it for publication was Lin Zhang.

fundamental role in the current density distribution across their cross-section that is the proximity effect. As one of the results of such a complexity caused by the simultaneous manifestation of the skin and proximity effects, any analytical approach becomes unfeasible, making the numerical approach to be the only way to be adopted.

Thus, amongst the various existing numerical methods to be applied is the method presented in [13] and in [14] with a matrix solution for the integral equation that rules the current density distribution across the section of a conductor, on which this work is based due to its didactic nature as well as its simplicity and fast convergence. In this way, this work starts with a theoretical explanation for the application of this integral method to the analysis of the behavior of the same infinitely long rectangular flat bar that is presented in [13] for playing the role of calibration for the subsequent application of the method. Thus, thanks to the successful result in the calibration stage, this same integral method was applied to some different theoretical configurations of rectangular conductors by culminating with the analysis of the behavior of a three-phase bus bar arrangement for which experimental data was taken for comparison.

Overall obtained results show that the application of the method is more adequate to planar configuration of conductors, in which the value of conductors' length is greater than the value of any other of their geometrical dimensions [15]. Another important result is that even in cases when the planar configuration is assumed any minor expected symmetry exists in the current density distribution over the cross-section of the conductors of a three phase arrangement. This important result indicates that designing of high-current equipment, device or system does require the adoption of specific software for properly evaluating the influences of the skin and the proximity effects in the inherently complex geometry of interleaved and curved conductors, as in panels bus bars, for example.

At last, the results of this work contribute to bridging an insisting gap in the knowledge of the skin effect, since the adopted method shows itself as being easy to be applied in the analyses of several basic theoretical cases [16]. In other words, this method serves itself as a feasible option for those who are involved in this theme and aim in increasing their knowledge farther than the classical analysis of an isolated circular conductor towards the analyses of real, complex, and practical cases, like those widely found in the industry.

The contributions of this paper for the study of skin effect are summarized in the following:

- The main contribution is related to the need for a better presentation of the skin effect on conductive busbars, in which there is no widespread knowledge about this model.
- The second contribution is related to show that the skin effect and the proximity effect play a decisive role in the distribution of current density across the cross-section panel power bus conductors.

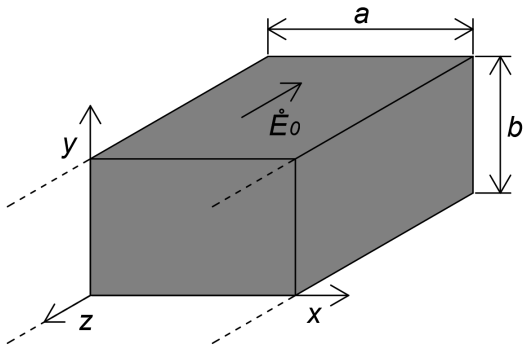

FIGURE 1. An infinitely long rectangular conductor submitted to a sinusoidal electric field uniformly distributed over its cross-section and towards the negative z coordinate. The angular frequency is in the power frequency range.

- The third contribution is related to the preponderance of the proximity effect in relation to the non-uniformity of the conductors. In this way, this method proves to be a powerful tool to spread knowledge about planar configurations, which are very useful to form the knowledge base that will allow the analysis of practical cases.

The advantages of the proposed method are: It has no difficulties in dealing with an analytical solution, it is intuitive and easy to implement the method, its results are accurate, and it is ideal for flat configurations. The disadvantages of the evaluated method are: For three-dimensional approaches, the significant increase in its complexity is sufficient to consider another numerical method to be applied, the cross-section ratification follows some restricted criteria, the analytical methods are appreciated for being elegant, but are intangible in this case.

This paper is organized as follows: In Section II, the theoretical background is presented to support the concepts regarding the skin effect. In Section III, the theoretical examples of some applications are presented. In Section IV, the results of the application of the adopted method are presented and discussed. Finally, the conclusions are discussed in Section V.

II. THEORETICAL BACKGROUND

Initially, by taking [13] as a reference, consider an infinitely long rectangular conductor of a homogeneous material, with width a and thickness b, steadily submitted to a uniform phasor electric field, $\dot{E}_o$, with angular power frequency w driven along its longitudinal axis. No other conductor is close enough to cause any influence on this rectangular conductor. At a certain point of this infinite conductor, a cartesian coordinate system is laid with the xy-plane on its cross-section, as shown in Fig. 1.

This same geometry can be applied to a vast number of study cases, ranging from designing of induction motors bars as in [4], [17] and [18] to human exposures to the magnetic field, as in [19]. Thus, for evaluating how the consequent current density is distributed over the cross-section of this conductor it is assumed as being formed by an array of $m \times n$

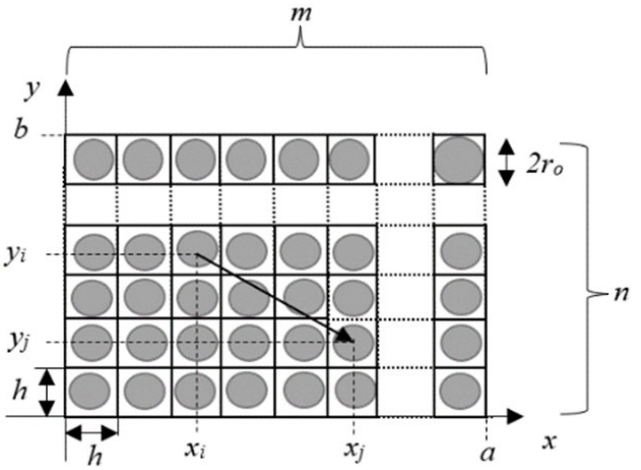

FIGURE 2. The rectangular cross-section of the conductor of Fig. 1 is divided into *m* times *n* squares with side *h*, involving a certain amount of the total current. Each square is represented by a circular conductor with a diameter equal to *h*.

small and equal squares with side h, within which a defined amount of current flows.

In this case, m is equal to a/h whereas n is equal to b/h and both are integer. Moreover, consider every square as being represented by an equivalent circular conductor with a radius equal to $h/2$ that is smaller than the corresponding penetration depth, for enabling the current density to be uniform over the cross-section of each of the squares, for avoiding the skin effect to take place. This representation is shown in Fig. 2.

On the other hand, consider the phasor expression for the magnetic vector potential over the radial distance, $\dot{A}(r)$, for a circular conductor of radius r_o, submitted to a phasor current, $\dot{I}$, that is

$$\dot{A}(r) = \frac{\mu_o \dot{I}}{2\pi}\left[\frac{1}{2} + ln\left(\frac{r}{r_o}\right)\right]. \quad (1)$$

For which r is the radial distance to the central axis of the circular conductor and μ_o is the magnetic permeability of the conductive material that is assumed to be the same as of the air. Thus, by assuming those same premises as in [13], the value of the phasor current density at a certain square on the cross-section of this conductor, $\dot{J}_{i=1,m.n}$, can be approximately evaluated through:

$$\dot{J}_{i=1,m.n} = -j\frac{\omega\mu_o}{2\pi}h^2 \sum \dot{J}_{j=1,m.n} \quad ln\left(r_{i,j}\right) + \sigma\dot{E}_o \quad (2)$$

in which besides those already described items, i corresponds to the square under evaluation, j corresponds to each of all the other squares of the cross-section, ω is the angular power frequency of the involved sinusoidal phasors, σ is the electrical conductivity of the conductor material and $r_{i,j}$ is the shortest distance between the i-th and the j-th squares centers, as indicated in Fig. 2 and given by

$$r_{i,j} = \sqrt{\left(x_i - x_j\right)^2 + \left(y_i - y_j\right)^2} \quad (3)$$

for which (x_i, y_i) and (x_j, y_j) are the respective coordinates of the center point of the i-th and the j-th squares, respectively. Still, as it is proofed in [13], for the case of $i = j$, this distance becomes

$$r_{i=j} = 0.47705\ h. \quad (4)$$

Thus, by taking advantage of the providentially chosen array structure for representing the conductor's cross-section, (2) can be arranged in a matrix form

$$\left[\dot{J}_{m\times n}\right] = \left[k_{m\times n,\ m\times n}\right]\left[\dot{J}_{m\times n}\right] + \sigma\left[\dot{E}_o m\ \times\ n\right] \quad (5)$$

for which $\left[\dot{J}_{m\times n}\right]$ and $\left[\dot{E}_o m\ \times\ n\right]$ are column matrices and $\left[k_{m\times n,m\times n}\right]$ is given by

$$\left[k_{m\times n,m\times n}\right] = -j\frac{\omega\mu_o}{2\pi}h^2\left[ln\left(r_{i=m\times n,j=m\times n}\right)\right] \quad (6)$$

as in [13] and presented in the script of a developed *Matlab* program.

In this sequence, the evaluation of the current density in every square $\dot{J}_{m,n}$ is performed after the following algebraic operation

$$\left[\dot{J}_{m\times n}\right] = \left\{[\,I\,] - \left[k_{m\times n,m\times n}\right]\right\}^{-1}\sigma\left[\dot{E}_o m\ \times\ n\right] \quad (7)$$

in which $[I]$ is a $(m \times n) \times (m \times n)$ identity matrix. These described steps enable the numerical evaluation of the current density over the whole conductor's section as it will be presented through some exemplifying selected cases before a practical case may be analyzed.

A. CURRENT APPLICATIONS

Currently, the skin effect is studied in several applications involving electrical engineering. This effect is present in Coaxial Conductors and there are several computation methods and mathematical models that confirm the correctness of the measurements of these signals [15]. Donaghy-Spargo and Horsfall [7] proposes an evaluation applied to power electronics. In their work, they describe the transient electromagnetic phenomenon specifically in electrical conductors that are connected to modern circuits. The effect is evaluated in transient operating regimes to describe the consequences.

A specific application for braking torque is presented in [20] as an important evaluation for heavy vehicles in relation to the performance parameters of a permanent magnet, where a comparison of the applied finite element method (FEM) is presented. The results presented in the work show that the simulation of the model for air gap flow density is in accordance with the values calculated through the FEM. The FEM stands out for several applications including evaluating the skin effect, as shown in [21]–[24]. In addition, for an accurate assessment through FEM, many authors emphasize the importance of considering this effect [25]–[27].

Lakhdari, Cheriet, and El-Ghoul [28] propose a study to conductive material thickness estimation from the analysis of the skin effect in non-destructive eddy current tests. In [29] a mathematical evaluation is proposed for numerical simulation of the skin effect and its consequences resulting from certain types of wires.

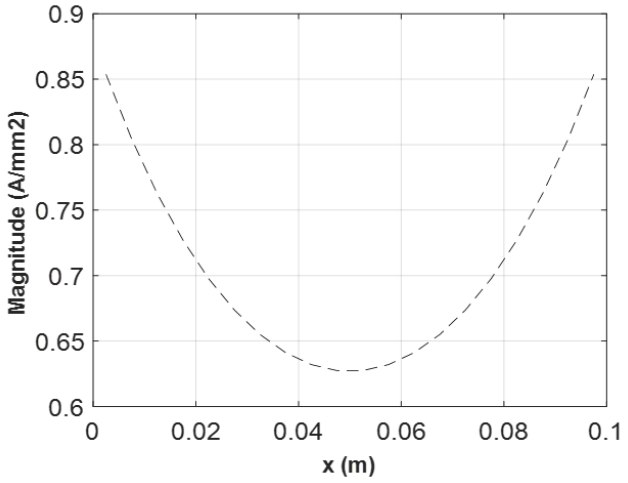

FIGURE 3. Amplitude phasor current density distribution over the bar width.

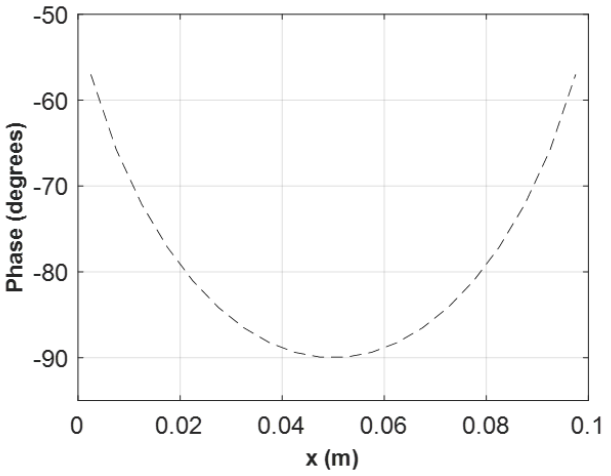

FIGURE 4. Phase angle phasor current density distribution over the bar width.

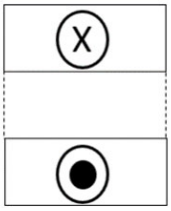

FIGURE 5. Cross-section view of the arrangement with two aluminum bars. An inward electric field in the upper bar and outward in the lower.

III. THEORETICAL EXAMPLES OF APPLICATION

Based on the proposed application of the method, some theoretical cases with different degrees of practical characteristics are simulated and their results are presented. These cases range from a very simple conductive flat bar to an elementary three-phase combination of bars and have been inspired in cases presented in [11].

Case 1: An infinitely long and flat 100 $mm \times 5$ mm aluminum bar is subject to a uniform and steady phasor electric field – This basic case has been already analyzed and results given in [13]. In this work, the presentation of that same analysis aims to calibrate the adoption by the authors of this same method.

For doing this, a simulation was performed for the bar modeled by 5 $mm \times 5$ mm ($h2 = 25$ $mm2$) squares with electrical conductivity of 35.3 MS/m, submitted to a 60 Hz phasor electric field uniformly distributed over its cross-section and driven along its longitudinal axis and thus over the negative values of z, with amplitude of 0.1 V/m and zero degrees as the phase angle, which gave origin to a total current with an amplitude of 347.34 A and $-78.1°$ as the phase angle.

Graphics of Figs. 3 and 4 respectively show the behavior of the phasor current density amplitude and phase angle over the bar width, represented by x ranging from 0 to 100 mm. In this case, it is important to emphasize one of the essential principles of the analysis that is the electric field as being uniformly imposed over the conductor's cross-section, whereas the distribution of the current density is the consequence.

This condition is significantly realistic since this is exactly what happens when panel bus bars are put in operation, for example. Still, from Fig. 4 it is possible to understand how inductive the total current is due to the range of negative values for the phasor current density, in comparison to the phase angle of the imposed electric field set to zero. This result means that the bus reactance predominates over its electric resistance, as numerically confirmed by the obtained value of $(59.4 + j281.71)\mu\Omega/m$ for the internal impedance per meter of this bus bar.

These so obtained results are equal to those of [13], which not only validates the implementation by the authors of the so adopted method as well as motivates the application of this same method to further cases, with some practical nature and that require to evaluate the mutual influences of the current density of nearby conductors, known as the proximity effect that can be understood as being an extension of the skin effect.

Case 2: Two identic, infinitely long 100 $mm \times 5$ mm aluminum bars have their width and length aligned, separated by a 5 mm air gap and each subject to a uniform 60 Hz phasor 100 mV/m electric field with opposite orientation to the other, as schematically shown in Fig. 5.

In response to the uniformly distributed applied electric field, the phasor current of each bar naturally flows in an opposite orientation to the other and the distribution of the phasor current density over the width of the bars behaves as shown on the graphics of Figures 6 and 7.

The computed current in each bar has an amplitude of 249.64 A and -81.2 degree as phase angle for the inward current and $+180 - 81.2 = +98.14$ degree for the outward current.

Comparison of this case with Case 1 allows concluding that for the same value of the applied electric field, current density becomes more uniform than for Case 1, although the value of the amplitude is lower, on average, which makes the value of the amplitude of the total current to be rather lower.

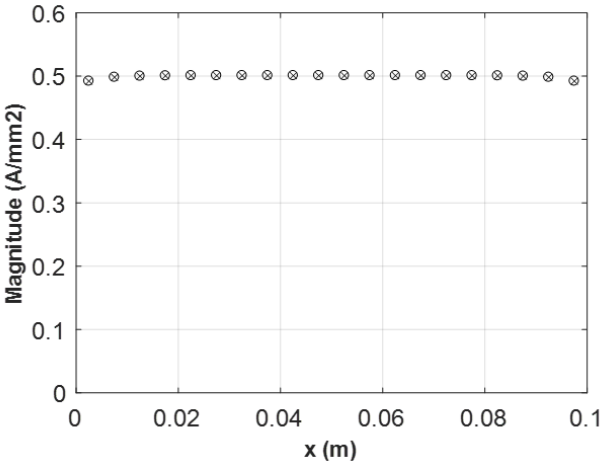

FIGURE 6. Amplitude phasor current density distribution over the width of the bars. (x) Inward and (o) outward.

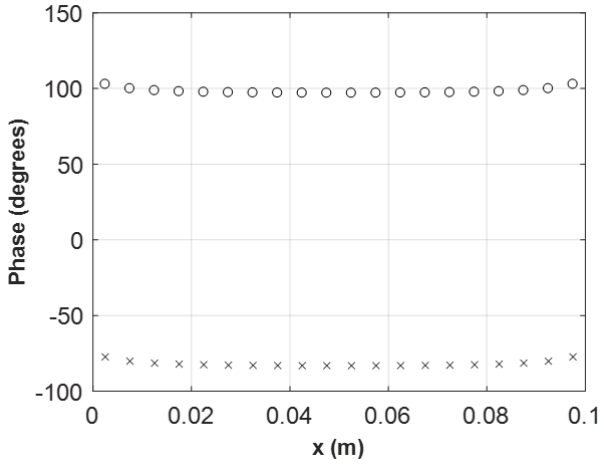

FIGURE 7. Phase angle phasor current density distribution over the bars width. (x) Inward and (o) outward.

These important results indicate that this kind of configuration of bars allows the better use of the conductors, thanks to the obtained uniformity of the current density amplitude. On the other hand, it is a fact that there is an increase in the value of the internal impedance per unit of length.

Case 3: Three identical, infinitely long 100 $mm \times 5$ mm aluminum bars have their height and length mutually aligned, separated by two 5 mm air gaps, and each bar is subject to an inward, uniformly distributed 60 Hz three-phase and 120 degrees balanced phasor 100 mV/m electric field, as schematically shown in Fig. 8, whereas Figures 9 and 10 show the behavior of the current density over the height of the bars.

Simulation results for such this application of a balanced three-phase phasor electric field of 100 mV/m with zero(left), -120 (center) and $+120$ (right) degree as phase angles generated respective currents with amplitude of 214.56 A and -71.06 degree as phase angle for the left bar, 245.41 A and 150.3 degree for the center bar and 278.56 A and 36.97 degree for the right bar.

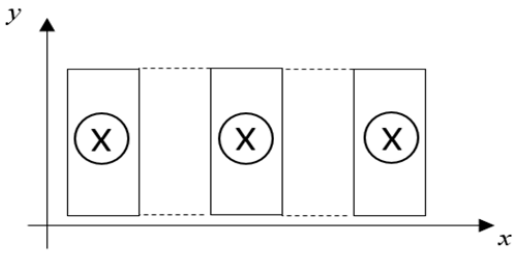

FIGURE 8. Cross-section view of the arrangement of the three aligned aluminum bars submitted to a balanced three-phase electric field.

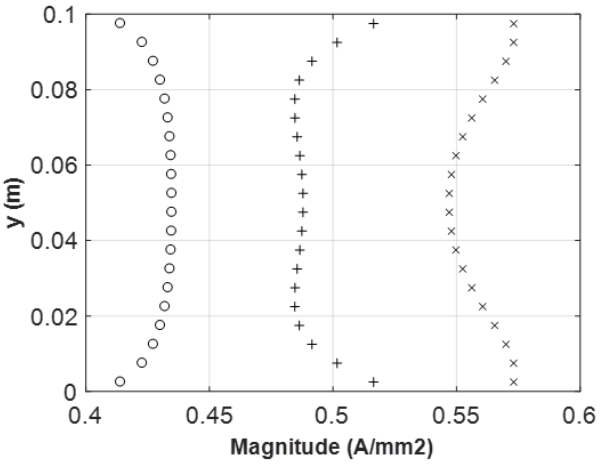

FIGURE 9. Amplitude phasor Current density distribution over the bars' height. (o) left bar, (+) center bar, (x) right bar.

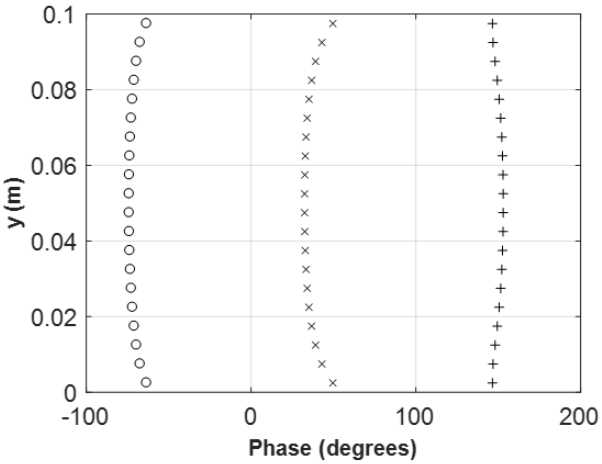

FIGURE 10. Phase angle phasor Current density distribution over the bars' height. (o) left bar, (+) center bar, (x) right bar.

In this case, an interesting result that the bar currents are neither balanced nor symmetrical. Yet, the phasor sum of the bar currents is not zero, which means that a return current, with an amplitude of 116.92 A and 47.47 degrees as phase angle is supposed to flow through an infinite path to return to the electric field source.

Now, as the last theoretical case to be studied and for characterizing the proximity effect, the mutual ability of two aligned bars in inducting current density is evaluated

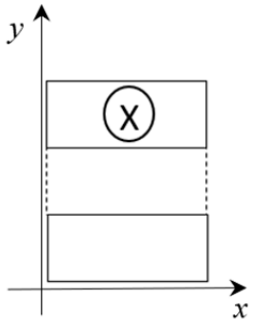

FIGURE 11. Cross-section view of the arrangement with two aluminum bars. An inward electric field in the upper bar and interrupted bar below.

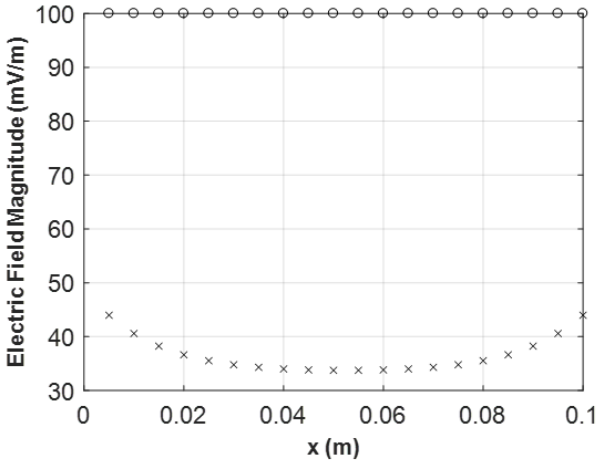

FIGURE 12. Electric field phasor module distribution over the width of the bars. (o) upper bar and (x) lower bar.

through the distribution of the induced electric field of the cross-section of a bar through which no current flows.

Case 4: Two identical, infinitely long aluminum bars 100 *mmx*5 *mm* are vertically aligned, separated by a 5 *mm* air gap. One of them is subject to a uniform 60 *Hz* phasor 100 mV/m electric field whereas the other is considered as being interrupted, which makes the current density to be null in it. Bars arrangement is as similar as in Case 2 and it is schematically shown in Fig. 11.

In this case, since the current density is set as null within the lower bar for it being interrupted, the distribution to be evaluated is that for the current density over the cross-section of the upper bar as well as that for the induced electric field over the cross-section of the lower bar.

Figs. 12 and 13 show the behavior of the module of electric field and current density phasor distribution over the width of the respective bars.

IV. A PRACTICAL EXAMPLE OF THE APPLICATION OF THE ADOPTED METHOD

For checking the applicability of the numerical method proposed in [13] for practical cases, based on a geometry proposed in [30] and inspired in [10], a commercially available panel bus bar was taken for running some laboratory tests.

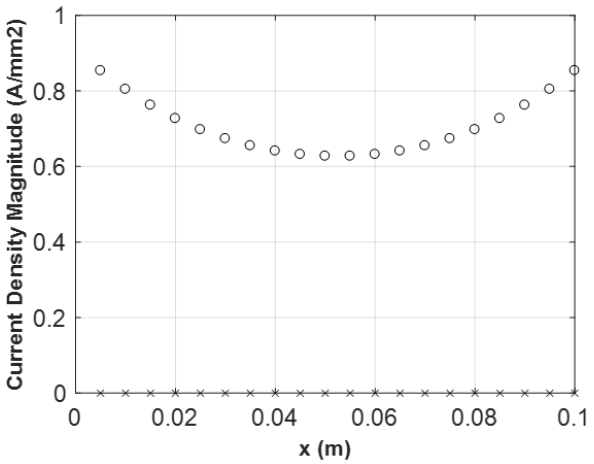

FIGURE 13. Current density phasor module distribution over the width of the bars. (o) upper bar and (x) lower bar.

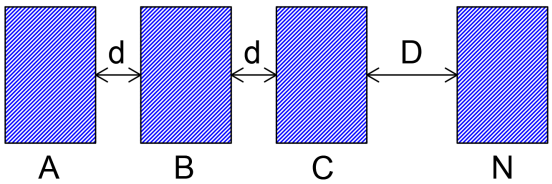

FIGURE 14. Cross-section view of the tested panel bus bars.

FIGURE 15. Upper view of the test set up for voltage application of bus bar laid on supports.

This panel bus bar is composed of 4 identical and paralleled 460 *mm* long copper bars, phase A, B, C and neutral, N, with electric conductivity $\sigma = 58\ MS/m$, as schematically shown in Fig. 14, with a width of 9.9 *mm*, the height of 33 *mm* and distance of d = 66 mm between any two consecutive phase bars whereas the neutral bar is $D = 118\ mm$ distant from phase C bar.

The tests were performed through the application of three-phase low voltage from a multi-tap $600-441-399-381-300-249-201-150\ V/3\ V (15\ kVA)$ transformer to the star connected short-circuited phase bars, without involving the neutral bar, as it is shown in Fig. 15, in which the measurement apparatus is also presented as well as the energy analyzer *Embrasul RE*6000 that was deployed for power and bar current measurements through its Rogowski's flexible probes.

TABLE 1. Experimental values.

Phase	Current (A)	Voltage (V)	Losses (W)	Apparent Power (VA)
A	616.50	0.101	14.21	62.27
B	604.2	0.108	32.84	65.53
C	588.3	0.126	22.52	74.25

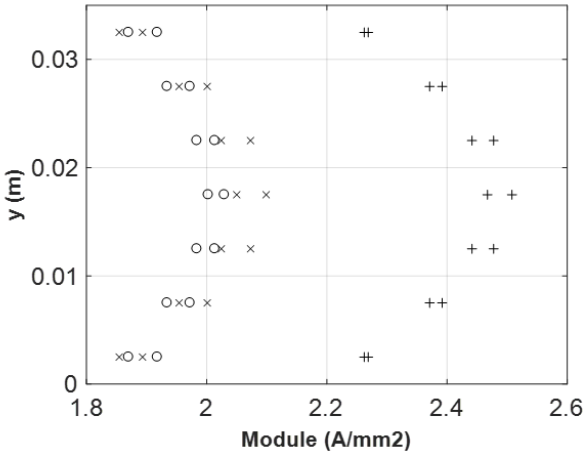

FIGURE 16. The amplitude of phasor current density distribution over the bars' height. Computer simulation (o) A, (+) B, and (x) C.

Results of measurement of the voltage across bar length, current, losses in the bars, and total apparent power after the current could stabilize and the bars could warm-up are shown in Table 1. In addition, for the measurement of voltage across each bar, a $6\frac{1}{2}$ digital multimeter *Agilent* 34401*A* was deployed.

In addition to the results of Table 1, the induced voltage across the neutral bar length was measured as 6.3 mV. Regarding power measurement, it could be evaluated after performing two different tests. The first one, with bars with rated current and a second one without the bars but with the flexible copper cordages star connected and with the same rated bus bar current. Thus, the difference in the results of these two tests represented the apparent, the active, and the reactive power of the busbars.

Thus, for performing the computer simulation of the experimental test, values of the column of voltage, in Table 1, were divided by the value of bars length, 46 cm, for obtaining the value of the applied electric field per phase, giving origin to values of the amplitude of 220 mV/m for the phase A, 234.8 mV/m for the phase B and 274 mV/m for the phase C, which is not a balanced set of three-phase phasors.

Nevertheless, the electric field three-phase phasors were supposed to have 120 degrees between each two of them. Due to condition in maintaining the square side, h, as uniformly applied, each of the bars was represented by a 10 mm of width $\times 35$ mm of height bar, separated by a distance of $D = 65$ mm. Results of this simulation are resumed in the graphics of Fig. 16 and in Table 2.

For obtaining the values of Table 2, the current density was integrated over the cross-section of each of the three bars by resulting in the phasor current. Thus, by multiplying the phasor voltage of each bar by the conjugate of the corresponding obtained phasor current, the phasor value for the apparent power was evaluated per bar. Each step of this evaluation can be seen on the *Matlab* script.

TABLE 2. Simulation values.

Phase	Current (A)	Losses (W)	Apparent Power (VA)
A	678.4	0	68.5
B	669.2	23.5	72.3
C	816.1	14.4	102.9

A. ANALYSIS OF THE RESULTS

The results obtained from the application of the adopted method for analyzing the behavior of the skin and the proximity effects under power frequency presented themselves as being as relevant and coherent. At first, the analysis of the same theoretical case presented in [13] was successfully reproduced, which allowed not only calibrating the application of the proposed methodology as well as enabled its application to different cases with gradually increasing practicality, inspired in [10] and [30]. Thus, the case of two parallel bars with the electric field longitudinally applied in opposite directions was analyzed and showed how the skin effect and the proximity become somehow canceled, whereas the impedance of the so combined bars increases significantly.

In extension, a theoretical case of a three-phase bars arrangement was analyzed, and its most interesting result was the surprising asymmetry of the current density distribution across the bars cross-section in respect to the central phase bar, represented by the graphic of Fig. 9. In principle, one could naturally expect a significant symmetry. Nonetheless, any symmetry happened neither for the amplitude nor for the phase angle of the phasor current density distribution over the bars' height.

Yet, with the aim of showing the key role played by the proximity effect, the distribution of the longitudinally induced electric field across the cross-section of an electrically interrupted bar was performed. The induced electric field was generated by the magnetic field created by the current longitudinally flowing in a similar and close parallel bar. For its turn, it is interesting to notice how the distribution of induced electric field along the interrupted close bar is not uniform over its cross-section. This studied case is unprecedented in the literature and it contributes for understanding the proximity effect in other cases than in bus bars, as in power transmission line cables [31]–[33], for example.

Indeed, among the most important results from these theoretical analyses, it should be mentioned how the proximity effect acts and predominates in the distribution of current density in the coupled and close conductors. At last, these so obtained results motivated the preparation of a practical experiment performed through the application of three-phase voltage to a short-circuited set of bars of a commercially available electric panel. Thus, this same case was modeled as much as possible and simulated by generating results for

the current density distribution that somehow resembles those from the practical experiment. Indeed, results for losses are rather different, although values of the amplitude of phase currents can be taken as being of the same level.

The main reason for the differences between theoretical and practical results relies on the assumption for the computer simulation that the bars are infinitely long whereas they are not only relatively short as well as there is a significant influence of the short-circuiting electric connections which have a length that is comparable to the bars, as can be seen on the photo of Fig. 14. Thus, these short-circuiting elements do cause multiple influences on the bars, enough to deeply modifying the results in comparison to the computer simulation.

Therefore, the planar nature of the method meets an applicability limit by indicating that three-dimension modeling is necessary, which can be performed through a commercially available finite element method program. Nevertheless, the theoretical results obtained do contribute for an increase in the knowledge of the skin effect under power frequency whereas experimental results can be taken as being good enough for motivating further analyses with simulating conditions as close as possible to those of practical cases, in which other incident elements cause influences in the current density distribution. For example, the panel walls made of steel and the unavoidable curves of the bars. Moreover, it is important to reinforce that this method serves as a potentially interesting tool for evaluating inductance values, magnetic field distribution and thermal effects [11] in circuits in which the values of the length of the involved conductors is the most significant dimension.

V. CONCLUSION

The application of the method of solution of integral equation [13] for modeling rectangle bars and theoretically evaluate the phasor current density distribution over their cross-section in power frequency has been shown as coherent and useful for different configurations of bars arrangement, providentially chosen for evidencing the skin effect in power frequency in this type of conductor.

This adopted method allows determining power frequency current density distribution across the cross-section of a conductor with any other geometry than the circular. Moreover, this method permits to consider the mutual influences of the magnetic field from carrying a current of close conductors, by evidencing the proximity effect and its key role.

By the way, the obtained results are usually mentioned as characterized as being the skin effect, although the proximity effect is the one that predominates. After simulating a set of providentially chosen theoretical cases, the comparison between a computer and an experimental simulation of a practical case of a set of panel bars has given promising evidence that more accurate results can be expected from the application of the method of the moments. With this aim, further studies shall be performed by considering the more intrinsically complex geometries of the bars than they simply paralleled aligned.

Moreover, the influence of and on the temperature distribution over the cross-section of each conductor is such a complex but necessary analysis to be done. Nevertheless, an interesting overall result of this work is that any of the expected symmetry of current density over the cross-section for the three-phase bars does not happen, which represents that changes in the conductor's cross-section geometry may happen and, in consequence, challenging opportunities for designing new panels bars arrangements are unveiled. In this case, the authors consider that some significant barriers may difficult the adopted method to be applied since concurrent methods indicate more convenient trade-offs.

The skin effect deserves attention considering that its existence represents losses in the system. The comparative analysis of the practical evaluation presented in this work could be compared with specific software simulation results such as those based on the finite element method, as discussed in the works related to this paper.

Indeed, the application of the method has taken the planar approach that is adequate for the cases of long conductors as found in power and distribution lines, since the border effects cause by field deflection can be neglected. For the cases when there are curves and short conductors, the complexity degree increases prohibitively enough to consider not only other approaches but another method. For example, finite elements.

ACKNOWLEDGMENT

The authors are thankful to the Coordination for the Improvement of Higher Education Personnel (CAPES), awarding a doctoral scholarship to one of the authors. Al Proyeto: Uso de algoritmos y protocolos de comunicación en dispositivos con énfasis en la privacidad de los datos.

REFERENCES

[1] L. J. Giacoletto, "Frequency- and time-domain analysis of skin effects," *IEEE Trans. Magn.*, vol. 32, no. 1, pp. 220–229, Jan. 1996, doi: 10.1109/20.477574.

[2] A. E. Kennelly, F. A. Laws, and P. H. Pierce, "Experimental researches on skin effect in conductors," *Trans. Amer. Inst. Electr. Eng.*, vol. 34, no. 2, pp. 1953–2021, Jul. 1915, doi: 10.1109/T-AIEE.1915.4765283.

[3] P. Wenlong, W. Xixiu, C. Shimin, and W. Shipu, "Preliminary study on the structure design of 330 KV GIS with three phase in one tank," *J. Eng.*, vol. 2019, no. 16, pp. 3092–3097, Mar. 2019, doi: 10.1049/joe.2018.8510.

[4] M. V. Terzic, D. S. Mihic, and S. N. Vukosavic, "Stator design and air gap optimization of high speed drag-cup induction motor using FEM," *Adv. Electr. Comput. Eng.*, vol. 13, no. 3, pp. 93–101, 2013, doi: 10.4316/AECE.2013.03015.

[5] T. Szczegielniak, Z. Piatek, B. Baron, P. Jablonski, D. Kusiak, and A. Pasierbek, "A discrete numerical method for magnetic field determination in three-phase busbars of a rectangular cross-section," *Turkish J. Electr. Eng. Comput. Sci.*, vol. 24, no. 3, pp. 1279–1291, 2016, doi: 10.3906/elk-1310-129.

[6] A. Canova and L. Giaccone, "Numerical and analytical modeling of busbar systems," *IEEE Trans. Power Del.*, vol. 24, no. 3, pp. 1568–1578, Jul. 2009, doi: 10.1109/TPWRD.2009.2014270.

[7] C. Donaghy-Spargo and A. Horsfall, "Transient skin effect in power electronic applications," *J. Eng.*, vol. 2019, no. 17, pp. 3696–3700, Jun. 2019, doi: 10.1049/joe.2018.8132.

[8] S. Cruciani, T. Campi, F. Maradei, and M. Feliziani, "Finite-element modeling of conductive multilayer shields by artificial material single-layer method," *IEEE Trans. Magn.*, vol. 56, no. 1, pp. 1–4, Jan. 2020, doi: 10.1109/TMAG.2019.2949737.
[9] W. Yin, J. Tang, M. Lu, H. Xu, R. Huang, Q. Zhao, Z. Zhang, and A. Peyton, "An equivalent-effect phenomenon in eddy current non-destructive testing of thin structures," *IEEE Access*, vol. 7, pp. 70296–70307, 2019, doi: 10.1109/ACCESS.2019.2916980.
[10] A. Ducluzaux, "Extra losses caused in high current conductors by skin and proximity effects," *Schneider Electr. Cahier Technique*, vol. 1, pp. 1–19, Jan. 1983.
[11] M. Kosek, M. Truhlar, and A. Richter, "Skin effect in massive conductors at technical frequencies," *Przegląd Elektrotechniczny (Elect. Rev.)*, vol. 87, no. 5, pp. 179–185, 2011.
[12] S. Li, Y. Han, and C. Liu, "Coupled multiphysics field analysis of high-current irregular-shaped busbar," *IEEE Trans. Compon., Packag., Manuf. Technol.*, vol. 9, no. 9, pp. 1805–1814, Sep. 2019, doi: 10.1109/TCPMT.2019.2910267.
[13] P. P. Silvester, *Modern Electromagnetic Fields: Time-Varying Fields in Conductors*, 1st ed. New York, NY USA: Prentice-Hall, 1968.
[14] W. Lipinski and P. Krason, "Integral equations methods of analysis describing the skin-effect in conductors," *IEEE Trans. Magn.*, vol. MAG-18, no. 2, pp. 473–475, Mar. 1982, doi: 10.1109/TMAG.1982.1061905.
[15] B. E. Fridman and M. V. Medvedev, "Skin effect in coaxial conductors of pulse facilities," *IEEE Trans. Plasma Sci.*, vol. 48, no. 2, pp. 482–490, Feb. 2020, doi: 10.1109/TPS.2019.2962214.
[16] F. Song, S. Yao, and Z. Wang, "Non-hermitian skin effect and chiral damping in open quantum systems," *Phys. Rev. Lett.*, vol. 123, no. 17, Oct. 2019, Art. no. 170401, doi: 10.1103/PhysRevLett.123.170401.
[17] J. D. Santiago, J. G. D. Oliveira, and H. Bernhoff, "Filter influence on rotor losses in coreless axial flux permanent magnet machines," *Adv. Electr. Comput. Eng.*, vol. 13, no. 1, pp. 81–87, 2013, doi: 10.4316/AECE.2013.01014.
[18] I. Vlad, A. Campeanu, S. Enache, and G. Petropol, "Operation characteristics optimization of low power three-phase asynchronous motors," *Adv. Electr. Comput. Eng.*, vol. 14, no. 1, pp. 87–93, 2014, doi: 10.4316/AECE.2014.01014.
[19] M. Costea, N. Golovanov, I. M. Grintescu, E.-L. Stanciulescu, and S. Gheorghe, "Human exposure to electromagnetic fields produced by distribution electric power installations," *Adv. Electr. Comput. Eng.*, vol. 14, no. 1, pp. 29–36, 2014, doi: 10.4316/AECE.2014.01005.
[20] W. Guo, D. Li, and L. Ye, "A model of magnetic field and braking torque in liquid-cooled permanent-magnet retarder accounting for the skin effect on permeability," *IEEE Trans. Veh. Technol.*, vol. 68, no. 11, pp. 10618–10626, Nov. 2019, doi: 10.1109/TVT.2019.2943414.
[21] S. An, B. Lee, Y. Bae, Y.-H. Lee, and S.-H. Kim, "Numerical analysis on the transient inductance gradient of the resistive overlay rail on the sliding electrical contact," *IEEE Trans. Plasma Sci.*, vol. 47, no. 5, pp. 2339–2342, May 2019, doi: 10.1109/TPS.2018.2889249.
[22] T. Campi, S. Cruciani, F. Maradei, and M. Feliziani, "Pacemaker lead coupling with an automotive wireless power transfer system," *IEEE Trans. Electromagn. Compat.*, vol. 61, no. 6, pp. 1935–1943, Dec. 2019, doi: 10.1109/TEMC.2019.2906328.
[23] S. Stefenon and A. Nied, "FEM applied to evaluation of the influence of electric field on design of the stator slots in PMSM," *IEEE Latin Amer. Trans.*, vol. 17, no. 4, pp. 590–596, Apr. 2019, doi: 10.1109/TLA.2019.8891883.
[24] S. F. Stefenon, L. O. Seman, C. S. F. Neto, A. Nied, D. M. Seganfredo, F. G. D. Luz, P. H. Sabino, J. T. González, and V. R. Q. Leithardt, "Electric field evaluation using the finite element method and proxy models for the design of stator slots in a permanent magnet synchronous motor," *Electronics*, vol. 9, no. 11, p. 1975, 2020, doi: 10.3390/electronics9111975.
[25] A. Namadmalan, B. Jaafari, A. Iqbal, and M. Al-Hitmi, "Design optimization of inductive power transfer systems considering bifurcation and equivalent AC resistance for spiral coils," *IEEE Access*, vol. 8, pp. 141584–141593, 2020, doi: 10.1109/ACCESS.2020.3013120.
[26] A. S. Kulkarni and J. M. Thomas, "Design of a pulsed alternator to drive a single-stage induction coilgun," *IEEE Trans. Plasma Sci.*, vol. 48, no. 10, pp. 3401–3408, Oct. 2020, doi: 10.1109/TPS.2020.3009219.
[27] D. Kaushik and M. J. Thomas, "Computational analysis of a pulsed power Source- based electromagnetic manufacturing process," *IEEE Trans. Plasma Sci.*, vol. 48, no. 10, pp. 3342–3349, Oct. 2020, doi: 10.1109/TPS.2020.3002021.
[28] A. E. Lakhdari, A. Cheriet, and I. N. El-Ghoul, "Skin effect based technique in eddy current non-destructive testing for thickness measurement of conductive material," *IET Sci., Meas. Technol.*, vol. 13, no. 2, pp. 255–259, Mar. 2019, doi: 10.1049/iet-smt.2018.5322.
[29] S. Gyimóthy, S. Kaya, D. Obara, M. Shimada, M. Masuda, S. Bilicz, J. Pávó, and G. Varga, "Loss computation method for litz cables with emphasis on bundle-level skin effect," *IEEE Trans. Magn.*, vol. 55, no. 6, pp. 1–4, Jun. 2019, doi: 10.1109/TMAG.2019.2890969.
[30] D. Kusiak, "The magnetic field and impedances in three-phase rectangular busbars with a finite length," *Energies*, vol. 12, no. 8, p. 1419, Apr. 2019, doi: 10.3390/en12081419.
[31] M. P. Corso, S. F. Stefenon, V. F. Couto, S. H. Lopes Cabral, and A. Nied, "Evaluation of methods for electric field calculation in transmission lines," *IEEE Latin Amer. Trans.*, vol. 16, no. 12, pp. 2970–2976, Dec. 2018, doi: 10.1109/TLA.2018.8804264.
[32] S. Ghosh, M. Ghosh, and S. Das, "Effects of multiple semiconducting screens on line parameters and wave properties of underground cable," *IEEE Access*, vol. 7, pp. 169371–169384, 2019, doi: 10.1109/ACCESS.2019.2955026.
[33] H. Chen, Y. Zhang, Y. Du, and Q. S. Cheng, "Lightning transient analysis of telecommunication system with a tubular tower," *IEEE Access*, vol. 6, pp. 60088–60099, 2018, doi: 10.1109/ACCESS.2018.2875723.

SÉRGIO H. L. CABRAL received the B.E. degree in electrical engineering (emphasis on power systems) from Universidade Federal Fluminense, in 1989, the M.E. degree in electrical engineering (high voltage and equipment) from the Federal University of Rio de Janeiro, in 1994, and the Ph.D. degree in electrical engineering (energy systems) from the Federal University of Santa Catarina, Brazil, in 2003.

Since 1994, he has been a full-time Professor-Researcher with the Regional University of Blumenau. His preferred areas of expertise in electrical engineering are related to the generation, transmission, and distribution of electric energy, high voltage and equipment, electrical grounding, transformers, induction machines, and electrical transients.

SÁVIO L. BERTOLI received the B.E. degree in chemical engineering from the Federal University of Santa Catarina, Brazil, in 1986, the M.E. degree in chemical engineering from the Federal University of Rio de Janeiro, in 1989, and the Ph.D. degree in mechanical engineering from the Federal University of Santa Catarina, in 2003.

He is currently a Professor with the Regional University of Blumenau. He has experience in the areas of physics and mathematics, with an emphasis on heat transfer, thermal, and thermodynamic processes, acting mainly on the following topics: heat transfer in multiparticle systems, analytical solutions to problems in transport phenomena, flow in the stokes regime, and processes advanced oxidation systems.

ALESSANDRO MEDEIROS received the B.E. degree in electrical engineering from the Regional University of Blumenau, in 2018, Brazil.

During his graduation he was a Monitor of Electromagnetism and Fundamentals of Engineering, a fellow of the Institutional Program for Initiation Scholarships in Technological Development and Innovation (PIBITI)/National Council for Scientific and Technological Development (CNPq) program, with the project of Static Converters applied in industrial electrical drives, guided by Prof. Sérgio Vidal Garcia Oliveira, and a fellow of the PIBIC / CNPq Program, with the study project of the Pelicular Effect in industrial frequency, guided by Prof. Dr. Sérgio Henrique Lopes Cabral.

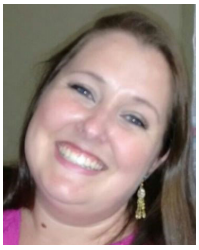

CRISLEINE REGINA HILLESHEIM received the B.E. degree in chemistry engineering from the Regional University of Blumenau, Brazil, in 2018, where she is currently the master's degree in chemical engineering.

CAROLINA K. DE SOUZA received the B.E. degree in food engineering from the Federal University of Santa Catarina, Brazil, in 2003, specialization in bromatology from the University of Ferrara, Italy, and the Ph.D. degree in chemistry and toxicology of foods from the University of Perugia, Italy, in 2008.

She was a Postdoctoral Researcher of Biochemical Engineering with the Federal University of Santa Catarina, in 2013. She is currently a Professor with the Courses of Food Engineering, Chemical Engineering, and Nutrition, and the Graduate Program in Chemical Engineering (PPGEQ), Regional University of Blumenau. She experience in food science with emphasis on food chemistry and functional foods. She operates in product development research lines, food preservation, and food safety. She is a member of the Human Research Ethics Committee.

STÉFANO FRIZZO STEFENON (Graduate Student Member, IEEE) received the B.E. degree in electrical engineering and the M.E. degree in electrical engineering (power systems) from the Regional University of Blumenau, Brazil, in 2012 and 2015 respectively. He is currently pursuing the Ph.D. degree in electrical engineering (artificial intelligence) with the Santa Catarina State University, Brazil.

He is currently developing research in artificial intelligence applied to the identification of faults in high voltage insulators with the Faculty of Engineering and Applied Science, University of Regina, Canada. He is also a Professor and a Coordinator of the undergraduate program of Electrical Engineering with the University of Planalto Catarinense. His work was focused on the classification of insulators, electrical inspections in the distribution networks, and artificial intelligence for fault identification in electrical power systems.

ADEMIR NIED (Member, IEEE) received the B.E. degree in electrical engineering from the Federal University of Santa Maria, Santa Maria, Brazil, in 1987, the M.E. degree in industrial informatics from the Federal Technological University of Parana, Curitiba, Brazil, in 1995, and the Ph.D. degree in electrical engineering from the Federal University of Minas Gerais, Belo Horizonte, Brazil, in 2007.

Since 1996, he has been a member of the faculty with the Santa Catarina State University, Joinville, Brazil, where he is currently an Associate Professor with the Department of Electrical Engineering. From August 2015 to July 2016, he was a Visiting Professor with the Wisconsin Electric Machines and Power Electronics Consortium, University of Wisconsin–Madison, Madison, WI, USA. His teaching and research interests include electrical machines, control of electrical drives, neural networks, and renewable energy.

VALDERI REIS QUIETINHO LEITHARDT (Member, IEEE) received the Ph.D. degree in computer science from INF-UFRGS, Brazil, in 2015.

He is currently an Adjunct Professor with the Polytechnic Institute of Portalegre and a Researcher integrated with the VALORIZA Research Group, School of Technology and Management (ESTG). He is also a collaborating Researcher with the following research groups: COPELABS, Universidade Lusófona de Lisboa, Portugal, the IT Branch Covilhã, Telecommunications Institute of Portugal, Portugal, the Department of Informatics, University Beira Interior, Covilhã, Portugal, the Laboratory of Embedded and Distributed Systems, University of Vale do Itajaí (UNIVALI), Brazil, and the Expert Systems and Applications Laboratory, University of Salamanca, Spain. His research interests include distributed systems with a focus on data privacy, communication, and programming protocols, involving scenarios and applications for the Internet of Things, smart cities, big data, cloud computing, and Blockchain.

GABRIEL VILLARRUBIA GONZÁLEZ received the M.Sc. degree in intelligent systems from the University of Salamanca, in 2012, the M.Sc. degree in internet security, in 2014, the M.Sc. degree in information systems management, in 2015, and the Ph.D. degree from the Department of Computer Science and Automation, University of Salamanca, Spain.

He was a Computer Engineer with the Pontifical University of Salamanca, in 2011. He is currently a Research Professor with the Department of Informatics. Throughout his training, he has followed a well-defined line of research, focused on the application of multi-agent systems to ambient intelligence environments, with special attention to the definition of intelligent architectures and the fusion of information.